COBEM 99
XV Congresso Brasileiro de Engenharia Mecânica
15th Brazilian Congress of Mechanical Engineering
22 - 26 de Novembro de 1999 / November 22 - 26, 1999 Águas de Lindóia, São Paulo,

AN INVESTIGATION INTO MECHANISMS OF LOSS OF SAFE BASINS IN A 2 D.O.F. NONLINEAR OSCILLATOR

Jessé Rebello de Souza Jr.
Miesher L. Rodrigues
Universidade de São Paulo, Departamento de Engenharia Naval e Oceânica
Av. Prof. Mello Moraes, 2231 - Cidade Universitária
05508-900 São Paulo, SP, Brasil

Abstract. *In this work we consider the transient stability of coupled motions of a 2 D.O.F. nonlinear oscillator that can represent, for example, the motions of a sea vessel under the action of trains of regular lateral waves. Instability is studied as the escape of the system from a safe potential well. The set of initial conditions in phase space that lead to acceptable motions constitutes its safe basin. We investigate the evolution of these safe basins under variation of parameters such as frequency and amplitude of waves, and an internal tuning parameter. Complex nonlinear phenomena are known to play an important role in determining the loss of safe basins as, say, wave amplitude is increased. We therefore investigate those processes, and attempt to classify them in terms of their speed relative to changes in parameter values. "Mechanism basins" are produced depicting regions of parameter space in which rapid or slow losses of safe basin are observed. We propose that a comprehensive understanding of mechanisms of loss of safe basins can be a valuable tool in assessing stability properties of these systems, and we give a conceptual view of how such information could be used.*

Keywords: *Nonlinear Dynamics, Nonlinear Stability, Escape Phenomena*

1. INTRODUCTION

Many physical systems have their dynamics largely determined by the interplay between "internal", potential forces, and "external" disturbance or excitation. Often, desirable motions take place inside potential wells, each one defined by a local minimum of some generalized potential function of, say, gravitational, elastic or electromagnetic nature. In such cases, system failure can be identified with the escape from a safe potential well, Thompson (1989). For a given level of external excitation some starting conditions inside the potential well will lead to safe, i.e., non-escaping trajectories whereas other starting points are associated to escaping behavior. Clearly, it can be of great practical interest to discern safe starting conditions from unsafe ones. A comprehensive answer to this question is, generally speaking, hopelessly difficult to obtain even in the simplest (but, of course, nonlinear) cases. From a practical point of view our attention would probably focus on "high energy" situations, where escape is more likely. But these are the conditions under which the full complexities of nonlinear dynamics are more likely to show up: coexistence of several attracting solutions, highly intertwined basins of attraction, fractal basin boundaries, etc. Also, the whole scenario will typically change as system parameters are varied, adding to the difficulty of generating a global picture of safe/unsafe dynamics.

A suitable example can be given by the 2 degree-of-freedom nonlinear oscillator that we shall consider in this work, see Thompson & de Souza (1996):

$$\begin{aligned} &\ddot{x} + 2\zeta\dot{x} + x - 2xy = F\sin(\omega t) \\ &\frac{2}{R^2}\left(\ddot{y} + 2\zeta R\dot{y}\right) + 2y = x^2 \end{aligned} \tag{1}$$

This oscillator, that we called the SIR (Symmetric Internal Resonance) model can be seen as a simple archetypal model of coupled heave-roll motions of a vessel acted upon by regular lateral waves. Here x and y are non-dimensional roll and heave displacements, respectively. A dot denotes derivative with respect to the non-dimensional time t. The damping ratio ζ represents the addition of linear viscous damping. The ratio of natural (linear) frequencies in heave and roll is given by R, which therefore acts as an internal tuning parameter. F and ω are parameters related to the amplitude and frequency of the incoming wave, respectively.

The SIR model contemplates two basic resonance mechanisms. Direct roll resonance is achieved when the wave frequency is close to the natural frequency in roll (in the non-dimensional form (1) that would be $\omega \approx 1$). Internal resonance is due to heave-roll coupling. To see that, let us set R = 2, and suppose that response in roll is harmonic at its natural frequency: $x = \sin(\omega t)$. The right-hand side of the heave equation will then be proportional to $\cos(2t)$, inducing large heave oscillations at twice the natural frequency in roll. This oscillation feeds back into the roll equation (through y), and because it multiplies x it constitutes a parametric excitation. Being at twice the natural roll frequency, it induces the principal Mathieu instability.

This oscillator exhibits a variety of steady-state attracting solutions that include various periodic responses as well as quasi-periodic and non-periodic (chaotic) behavior. A sample bifurcation diagram depicting the so-called main sequence is shown in Fig. 1. This bifurcation diagram is obtained through an attractor-following technique starting at $x = \dot{x} = y = \dot{y} = F = 0$ and determining the evolving steady-state responses as the magnitude of forcing F is slowly increased for a fixed wave frequency ω. For the wave frequency $\omega = 0.85$ the evolution of attracting steady-states from rest can be summarized as follows. For small F the system exhibits periodic response with the period of the forcing. At around $F = 0.1380$ the system goes through a supercritical Neimark bifurcation, settling onto a resonant quasi-periodic motion. Further increase in F will increase the amplitude of quasi-periodic motions until, at around $F = 0.1385$, the systems goes through the first of a series of saddle-node bifurcations. For F in the range between 0.14 and 0.18, the amplitude of motion varies relatively little, but the system goes through a complex cascade of saddle-node bifurcations (map explosions) in which periodic windows are interspersed among regions of quasi-periodic response. Just before $F = 0.18$ a relatively long period-21 response settles in at a further saddle-node bifurcation. At around $F = 0.185$ a saddle-node bifurcation (intermittency explosion) destroys the stability of the periodic attractor, resulting in stable motions of apparently chaotic nature. Chaotic behavior predominates until shortly after $F = 0.2$, when escape occurs at a blue-sky catastrophe.

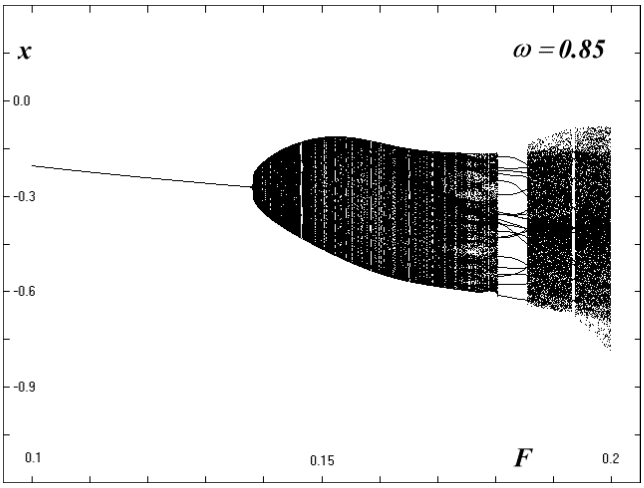

Figure 1. Bifurcation diagram of the main sequence for the SIR model with
$\zeta = 0.05, R = 1.7, \omega = 0.85$

Although useful, bifurcation diagrams only tell part of the story. For any given combination of control parameters (ζ, *R*, *F*, ω) a number of attracting solutions will typically coexist, their basins of attraction splitting the phase space (of starting conditions) among them. For example, in Fig.1 a wide periodic window is clearly seen around *F* = 0.184. However, this period-21 response is not the only bounded attracting solution for this condition; there exists a competing non-periodic (chaotic) attractor not captured by attractor-following the main sequence.

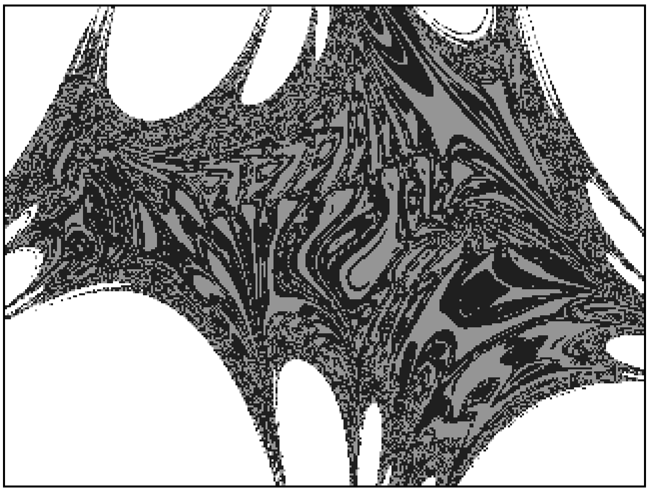

Figure 2. Basins of attraction for the SIR model; box coordinates are: $-1.2 < x < 1.2$ (horizontal), $-1 < y < 1$ (vertical), $\dot{x}(0) = \dot{y}(0) = 0$, *F* = 0.184, ω = 0.85, *R*=1.7, $\zeta = 0.05$, color legend: black = non-periodic (chaotic), gray = period 21, white = escape.

Figure 2 illustrates the complex appearance of the highly intertwined basins of these two attractors. We can see in Fig.2 that although for this value of *F* the bulk of non-escaping trajectories still form a relatively “solid” region, fractal-like boundaries between escaping and non-escaping trajectories have already developed along the periphery of this region. These fractal tongues will, under further increase in F, sweep across the whole region (see also Fig. 3).

2. SAFE BASINS

The considerations presented in the Introduction exemplify the well-known fact that the details of steady-state dynamics of even simple oscillators can be overwhelmingly complex. Sometimes, however, such detailed knowledge can be of little meaning, perhaps even slightly misleading and at any rate unnecessary. Many systems operate under external disturbance that can vary both widely and rapidly. Clearly in such conditions there is no time for any significant steady-state to be achieved, and attractors are probably best regarded as rather loose underlying organizing features of the dominant transient dynamics. Also it is well known that looking directly at transient dynamics can be at the same time simpler and more relevant, see for instance Thompson & Soliman (1990). Simplicity comes from overlooking fine detail and concentrating on features of interest such as escape. Also, associating failure with the final disappearance of safe attractors can be non-conservative for their basins of attraction may be severely reduced well before the final collapse, see Thompson & de Souza (1996) and also the next section.

We therefore choose to look temporarily away from steady-state dynamics and its associated concepts of attractors and basins of attraction. Instead we define *escaping trajectories* as those that satisfy an appropriate escape criterion for some time t between zero and an upper limit for the transients considered. Escape criteria can be defined in various ways. They may be envisaged as a means to identify trajectories attracted to infinity (if they exist for the model) or to adjacent, unacceptable potential wells. Alternatively, and that is the approach we favor here, the escape criterion can reflect real-life constraints to the motions of the system. Therefore for the SIR model we shall label trajectories as escaping if they wander (a certain distance) beyond the symmetrically placed local maxima at $(x, y) = (\pm 1, 1/2)$. Note that these maxima represent the so-called angle of vanishing (static) stability, meaning that if the vessel is released in calm water with a heeling angle larger than that it will capsize statically.

Safe basins are defined as the union set of starting conditions $(x_0, \dot{x}_0, y_0, \dot{y}_0) = (x(0), \dot{x}(0), y(0), \dot{y}(0))$ such that escape does *not* occur for any $0 < t < t_f$. Of course, the size and shape of safe basins will depend on system's parameters, and it would be of interest to follow the evolution of safe basins as parameters are varied. Safe basins are objects of the same dimension of the phase space, four-dimensional in our case. Therefore they cannot be fully visualized here. Useful insight can however be derived from observation of two-dimensional cross-sections. These can be specified by keeping the initial value of two of the phase variables at zero, for example, $(\dot{x}_0, \dot{y}_0) = (0,0)$. We shall see shortly several examples of such cross-sectional safe basins, but for the moment let us just recall that these portraits can and will, just like basins of attraction, undergo very complex metamorphoses. Presumably (rigorous proofs are thin on the ground) such transformations are dictated by the underlying changes in steady-state features of attractors and their basins of attraction.

3. MECHANISMS OF LOSS OF SAFE BASINS

Typically there will be natural limits to the interesting values for the phase variables. Let us assume that a certain *window* in the space of initial conditions is defined for the SIR model, by $\lfloor x_{i_0} \rfloor_{\inf} \le x_{i_0} \le \lfloor x_{i_0} \rfloor_{\sup}$, where $i = 1,2,3,4$ and $(x_{1_0}, x_{2_0}, x_{3_0}, x_{4_0}) = (x(0), \dot{x}(0), y(0), \dot{y}(0))$. For any given point in the space of control parameters spanned by (ζ, *R*, *F*, ω), and for a given escape criterion, the *ratio* of safe to escaping starting conditions within that window is fixed. *Loss of safe basins* is the reduction of that ratio experienced by the system as one or more of its control parameters are varied. Obviously any change in control parameters can in principle have its effects investigated. For simplicity, we shall concentrate here on a specific mode of change, namely the increase of magnitude of forcing *F* for fixed values of the remaining parameters. That would emulate the loss of stability of a vessel in waves as more severe sea states are faced. By considering whole series of such evolutions we aim at drawing a first picture of the general stability behavior for this system. For that purpose we shall take $\zeta = 0.05$ and consider ranges of frequency ω and internal tuning parameter *R* centered on potentially interesting points (see Table 1 below).

As said before it is reasonable to suppose that the loss of (transient) stability can be related to underlying (steady-state) phenomena such as bifurcations. In fact, one objective of this study is to investigate that correlation. We shall suggest that certain relevant macroscopic features of processes of loss of safe basins can be related to broad classes of bifurcational phenomena. This correspondence inspires a classification of mechanisms of loss of safe basins in terms of their practical severity as measured by the swiftness of degradation of stability for increasing *F*.

For the present study we have carried out a systematic survey of loss of safe basins in which we have covered the ranges shown in Table 1.

Table 1. Ranges for numerical experiments of loss of safe basins

Parameter	Minimum	Maximum	Step
ω	0.5	1.3	0.1
R	1.0	3.0	0.2
F	0.0	0.4	0.05

Note that $\omega = 1.0$ corresponds to theoretical roll resonance, and $R = 2.0$ yields internal resonance. For each (R, ω)-pair, a sequence of nine safe basin portraits was generated (for *F* varying from 0.0 to 0.4 in steps of 0.05). Ninety-nine such sequences were investigated, as shown in Table 1, resulting in a grand total of 891 portraits. Each portrait was produced from a $(x, \dot{x}, y, \dot{y})$-grid of $160 \times 1 \times 120 \times 1 = 19200$ evenly spread starting conditions covering a window defined by $-1.1 \le x \le 1.1$, $-0.6 \le y \le 0.6$, $\dot{x} = \dot{y} = 0$. The escape criterion used was $|x| \ge 1.2$, and the maximum duration of transients was given by 10 cycles of the forcing function. A fourth-order Runge-Kutta integration algorithm was employed with a fixed step size of $1/20$ times the period of the forcing function.

It is not possible to reproduce here all 891 portraits used for the subsequent analysis. Instead, we show in Fig. 3 a selection of some sequences that we feel illustrate rather well the whole spectrum of processes of loss of safe basins observed. In Fig. 3 safe basins are depicted in black with white regions corresponding to escape. Perhaps the first feature to be noticed is that safe basins invariably develop very complex geometries as the energy level of the system – closely related to *F* – increases. There is little hope of capturing their evolution by simple formulae. Also due to the complexity of their shape, it is quite clear that no single point can be reliably used as a test-case for escape: it could always happen that safe basins shrink around such point leading to an overestimation of minimum amplitudes necessary for escape.

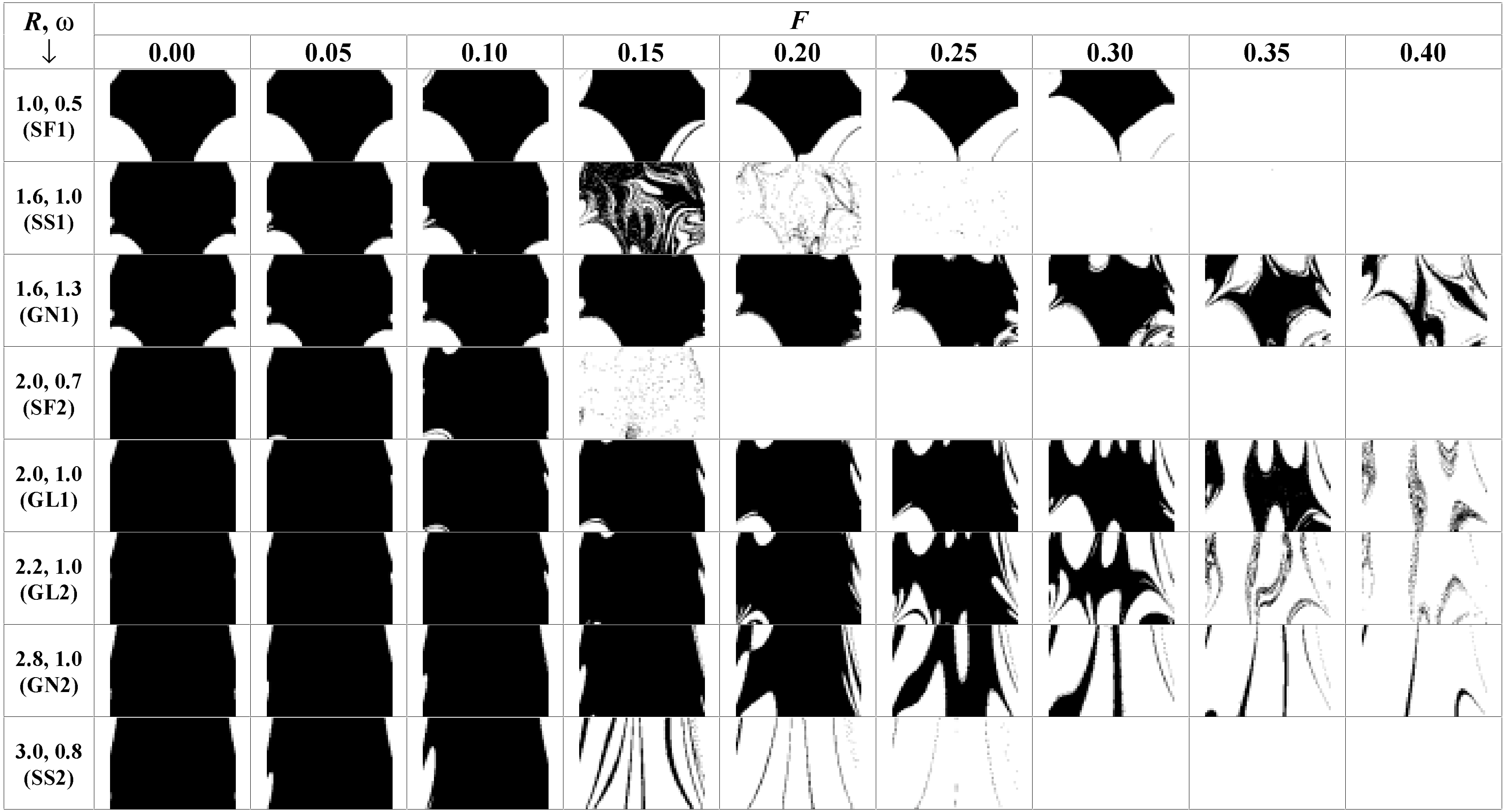

Figure 3. Sample sequences illustrating processes of loss of safe basins

The second observation that can be made from Fig. 3 is that severe loss of safe basin can take place at widely varying values of F and also at very different *rates*. We feel that both of these aspects – the value of F for severe loss of safe basin, and the rate of loss with respect to F – play a significant role in the practical study of the stability of these systems. The first of these aspects measures the amount of disturbance the system will endure without failing (escaping). The latter aspect gives an indication of how "robust" the above measure is. In other words, if we assume the system will be safe up to a certain magnitude F^* of forcing, it would be highly undesirable if shortly after F^* the bulk of the safe basin would quickly vanish. A *gradual loss of safe basins* would naturally be preferable.

As said above we would like to relate the broad features of loss of safe basins to underlying bifurcational phenomena. A systematic investigation of the (main) bifurcation sequences for the various (R, ω)-pairs suggested that, for practical purposes, processes of loss of safe basin could be broadly classified as *gradual* or *sudden*. For each of these categories, two different cases could be distinguished. Gradual loss of safe basin happens when either there is *no bifurcation* of the main sequence (i.e. the period-1 response remains attracting) or there is a relatively *long bifurcation sequence* in terms of its F-range, usually including wide spells of complex (high-order periodic or aperiodic, chaotic) motion. On the other hand, sudden loss of safe basin is typically associated either with a *fold bifurcation* (saddle-node jump to a remote attractor) or with a *short bifurcation sequence* in which only very brief intervals of any responses other than period-1 are discernible. The sequences depicted in Fig.3 were also chosen to exemplify each of the above cases, as shown in Fig.4, where their corresponding bifurcation sequences are also represented. For easy identification we have labeled the four cases with mnemonic acronyms followed by a number (1 or 2). Note that in Fig.3 we have also used these labels to identify the corresponding loss sequences shown there. So we have: <u>G</u>radual, <u>N</u>o bifurcation (GN1 and GN2); <u>G</u>radual, <u>L</u>ong bifurcation sequence (GL1 and GL2); <u>S</u>udden, <u>F</u>old bifurcation (SF1 and SF2); <u>S</u>udden, <u>S</u>hort bifurcation sequence (SS1 and SS2).

A few remarks should perhaps be made with regard to the loss-of-safe-basin/bifurcation-sequence correlation suggested by the above investigation. Firstly, the unsuitability of steady-state escape as a measure of system integrity (see also Thompson & Soliman (1990)) is clearly exemplified, particularly by the gradual loss sequences GN1 and GN2. In both these sequences safe basins are severely eroded well before $F = 0.40$ although the initial period-1 solution is still attracting. Secondly, there seems to be no direct link between the *F-value* at which severe loss of safe basin occurs and the *mechanism* that will be involved in it. For example, sequences SF1 and SF2 both illustrate a sudden loss of safe basin with underlying fold bifurcation but in SF1 a sizeable safe basin is retained up to $F \approx 0.30$, whereas in SF2 the safe basin has all but vanished at $F \approx 0.15$. Likewise, although *loss sequences* GL2 and GN2 are quite similar, developing at roughly the same rate (see Fig. 3), the underlying *bifurcation sequences* are totally diverse (see Fig. 4). Other examples can be extracted from inspection of Fig. 3 and Fig. 4. Thirdly, it seems difficult to ascribe the sudden (or gradual) loss of safe basin to one or other specific bifurcation or sequences of bifurcations of the underlying main sequence. It can be observed that whenever the main sequence undergoes a *fold* (saddle-node) bifurcation loss of safe basin is *sudden*. This is true even in sequence SS2, in which *after* the fold the system still undergoes a short bifurcation sequence finally leading to escape (but note that after the fold at $F \approx 0.10$ most of the safe basin is lost). However, as SS1 shows, a sudden loss of safe basin can also happen in the *absence* of a fold bifurcation (the bifurcation sequence in SS1 starts with a symmetry-breaking bifurcation before the system goes through a period-doubling cascade).

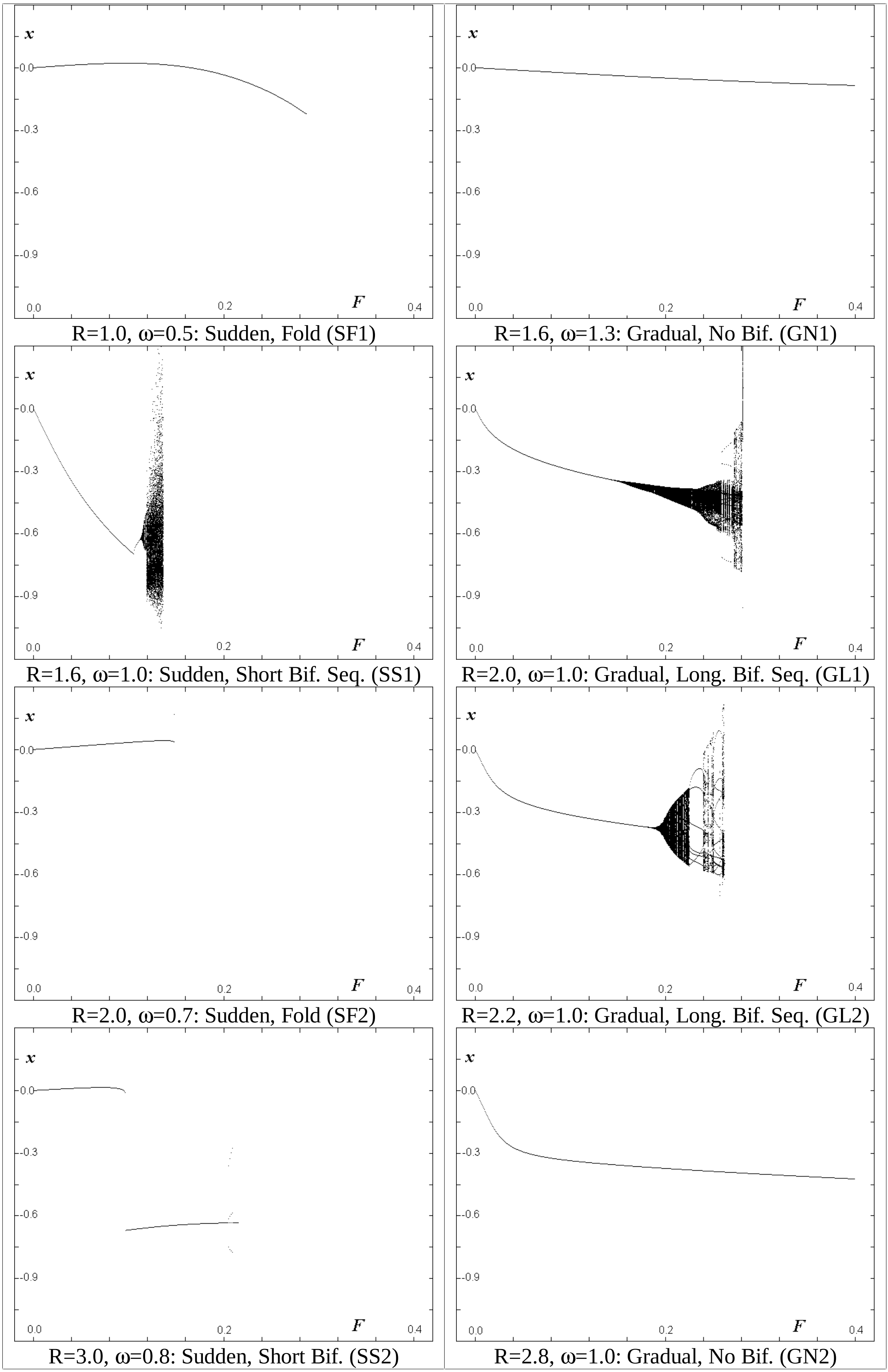

R=1.0, ω=0.5: Sudden, Fold (SF1)

R=1.6, ω=1.3: Gradual, No Bif. (GN1)

R=1.6, ω=1.0: Sudden, Short Bif. Seq. (SS1)

R=2.0, ω=1.0: Gradual, Long. Bif. Seq. (GL1)

R=2.0, ω=0.7: Sudden, Fold (SF2)

R=2.2, ω=1.0: Gradual, Long. Bif. Seq. (GL2)

R=3.0, ω=0.8: Sudden, Short Bif. (SS2)

R=2.8, ω=1.0: Gradual, No Bif. (GN2)

Figure 4. Bifurcation sequences corresponding to processes show in Fig. 3

4. MECHANISM BASINS

To conclude this brief exploration of processes of loss of safe basins we would like to have a global idea of how the sudden and gradual processes position themselves in the (R, ω)-plane. In order to quantify the swiftness with which safe basins are lost as the control parameter F is increased we take the same data used to produce the portraits shown in the previous section, and we introduce the Maximum Speed of Erosion σ, which we define for each (R, ω)-pair as:

$$\sigma = \max\left\{\frac{abs(S_{i+1} - S_i)}{F_{i+1} - F_i}, i = 1,2,\ldots,N-1\right\} \tag{2}$$

where S_i is the ratio of safe to total starting conditions within the window used, and the F_i are each one of the N discrete F-values used (see the previous section for actual values used in this study). Since $(S_{i+1} - S_i)$ is usually negative, we take them in absolute value. In Fig. 5, consistently with our choice of two levels of speed of loss (gradual or sudden), we color in dark gray sequences with σ larger than 10. Figure 5(a) shows a 3D view where relative values can be assessed, whereas Fig. 5(b) is a contour plot.

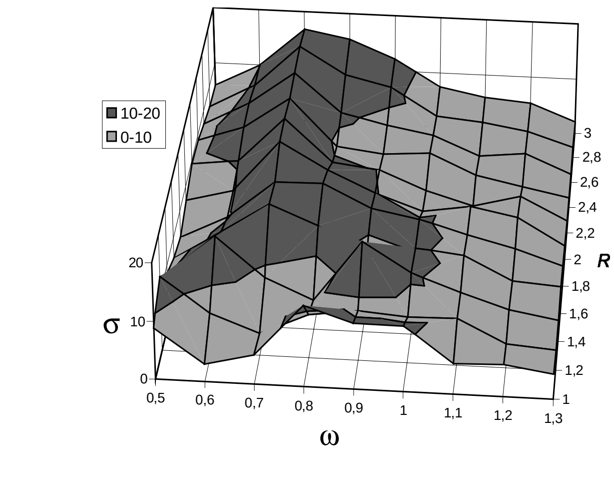

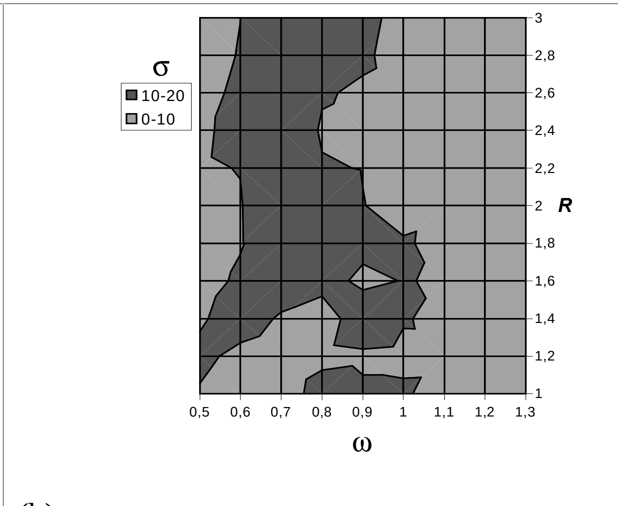

Figure 5. “Mechanism basins” depicting regions of gradual and sudden loss of safe basin

Perhaps the main conclusion that can be drawn from Fig. 5 is that sudden loss of safe basin is a *resonance phenomenon*. Whatever the precise underlying bifurcation sequences are, sudden loss tends to occur around the system’s resonant oscillations. The SIR model here investigated illustrates rather well this fact. For low values of R where both direct and internal resonance are relevant we see two peaks in the σ surface corresponding broadly to each of those resonant motions. For larger values of R the system behaves more like a 1 D.O.F. oscillator with roll motions following very closely the static solution in heave. And in this case only one peak of σ is observed corresponding to direct roll resonance (remember that the softening nonlinear restoring curve of the SIR model will cause roll resonance to shift towards lower values of ω).

5. CONCLUSIONS

We have carried out a systematic study on the mechanisms responsible for loss of safe basins of transient motions in a 2 D.O.F. oscillator. Several results were outlined based on the analysis of a rather extensive numerical investigation, including:

- Loss of safe basin can happen at different F-values and at different rates (which we have broadly classified into sudden or gradual).
- The speed of loss of safe basin is not directly related to the F-value at which severe loss starts.
- It seems to be possible to correlate sudden or gradual loss of safe basin with broad features of underlying main bifurcation sequences, but not with specific bifurcations.
- Sudden loss of safe basin tends to occur around conditions of either internal or direct resonance.

This investigation is part of a line of study whose objective is to develop simple, practical stability criteria for nonlinear oscillators. We feel that from a good understanding of how safe basins are eroded near critical conditions an expedient method can be envisaged. We have proposed elsewhere that a suitable grid of starting conditions can act as an adequate test for robust stability, de Souza & Bishop (1997), de Souza & Bishop (1998). Furthermore, we have proposed that only a small number of points need to be included in such grids provided they are adequately spaced inside the safe potential well. The results of the present study suggest that safe basins do not follow specific or simple geometries as they are eroded, encouraging the idea that a unique coarse grid could, in principle, offer a good estimate of F-values at which significant loss of safe basin has occurred.

REFERENCES

de Souza, J. R. & Bishop, S. R., 1997, Boundaries of safe operation of mechanical oscillators, Applied Mathematical Modelling, vol. 21, pp. 108-112.

de Souza, J. R. & Bishop, S. R., 1998, Boundaries of safe motion through a coarse grid-of-starts, Journal of the Brazilian Society of Mechanical Sciences, vol. XX, n. 4, pp. 564-575.

Thompson, J. M. T., (1989), Chaotic phenomena triggering escape from a potential well, Proceedings of the Royal Society London, vol. 421, pp. 195-225.

Thompson, J. M. T. & de Souza, J. R., 1996, Suppression of escape by resonant modal interactions: in shell vibration and heave-roll capsize, Proceedings of the Royal Society London, vol. 452, n. 1954, pp. 2527-2550.

Thompson, J. M. T. & Soliman, M. S., 1990, Fractal control boundaries of driven oscillators and their relevance to safe engineering design, Proceedings of the Royal Society London, vol. 428, n. 1954, pp. 1-13.